Materials Science & Engineering C 113 (2020) 111020

Contents lists available at ScienceDirect

Materials Science & Engineering C

journal homepage: www.elsevier.com/locate/msec

A new application of inorganic sorbent for biomolecules: IMAC practice of Fe^{3+}-nano flowers for DNA separation

Ayça Serinbaş[a], Burcu Önal[a], Ömür Acet[a], Nalan Özdemir[b], Volha Dzmitruk[c], Inessa Halets-Bui[c], Dzmitry Shcharbin[c], Mehmet Odabaşı[a,*]

[a] Chemistry Dept. Biochemistry Division, Faculty of Arts and Science, Aksaray University, Aksaray, Turkey
[b] Chemistry Dept. Biochemistry Division, Faculty of Science, Erciyes University, Kayseri, Turkey
[c] Institute of Biophysics and Cell Engineering of the National Academy of Sciences of Belarus, Minsk, Belarus

ARTICLE INFO

Keywords:
Copper phosphate nanoflowers
IMAC
DNA separation

ABSTRACT

Selection of purification method and type of adsorbent has high significance for separation of a biomolecule like deoxyribonucleic acid (DNA). Nanoflowers are a newly improved class of adsorbent. Due to showing very structural similarity to plant flowers, they are named as nanoflowers. Herein, after synthesize of copper phosphate three hydrate nanoflowers [$(Cu_3(PO_4)_2.3H_2O)$, CP-NFs], Fe^{3+} ions were attached to their surfaces. Obtained Fe^{3+}-CP-NFs, before investigation of some adsorption parameters for DNA, they were characterized by scanning electron microscopy (SEM), energy-dispersive X-ray (EDX), X-ray diffraction (XRD) and Fourier transform infrared spectroscopy (FTIR). Some attained data from the results of adsorption experiments as follows: While maximum DNA adsorption on Fe^{3+}-CP-NFs was found as an excellent value of 845.8 mg/g, nanoflowers without Fe^{3+} ions adsorbed DNA as only 25.3 mg/g. Optimum media conditions for DNA adsorption were observed at pH 7 and 25 °C with an initial concentration of 1.5 mg/mL DNA. Langmuir and Freundlich adsorption equations were applied to determine which adsorption model was appropriate, and it was seen that Langmuir model was fit with a R^2 of 0.9885.

1. Introduction

Separation of DNA is a common research in biological and medical applications [1], and adsorption of it has been widely studied on some surfaces for different applications such as the treatment of autoimmune illnesses [2], cloning procedure [3], gene therapy [4], DNA vaccination [5], molecular diagnosis of diverse sickness [6], etc. In the last decades, improving the efficient methods for DNA purification has been a desirable situation for many researchers since gene therapy, protection, and purification has a great importance with this aspect of DNA [7].

Nanoflowers are a newly improved class of tiny particles demonstrating structural similarity to plant flowers [8]. Especially, from the study of protein-inorganic hybrid nanoflowers reported in 2012 first, [9] to the present, researchers have shown great interest to perform them for not only biochemistry usage [10] but also environmental application such as dye decolorization [11], heavy metal removal [12] etc. When compared to other well-designed sorbents used by different groups [13–20], nanoflowers have a comparable level via adsorption capacity and remedy.

While a lot of studies including organic-inorganic systems such as $CaHPO_4$-α-amylase hybrid nanobiocatalytic system [21], combination of three pancreatic digestive enzymes [22] horse radish peroxidase (HRP)-nanoflowers [23], etc. were studied, organic-inorganic-organic systems (multi-enzyme process) such as glucose oxidase and horseradish peroxidase-nanoflowers [24] were also given to literature. Nanoflowers have large surface/volume ratio and abundant cavities, which can increase the efficiency of surface reactions compared to zero (0D), one (1D) and two (2D) size equivalents. And also, due to the micrometer size of the whole structure, they have fascinating properties such as superior catalytic efficiency, mechanical strength and easy recovery [25,26]. Although there are more applications of organic-inorganic studies on nanoflowers, use of pure inorganic nanoflowers for separation of biomolecules are limited.

The performance of surface reaction can be enhanced with 3D structure of nanoflowers because of increasing number of adsorption sites [8]. The excellent features of hybrid nanoflowers have offered a wide range of some different and challenging applications such as separation, biosensing, enzyme mimetics, catalysis, coating and energy storage [26,27]. Since multifunctional hybrid nanoflower systems have not been completely discovered, nanoflower systems still need to be explored [10].

* Corresponding author at: Aksaray University, Faculty of Arts and Science, Chemistry Department, Biochemistry Division, 68100 Aksaray, Turkey.
E-mail address: modabasi@aksaray.edu.tr (M. Odabaşı).

https://doi.org/10.1016/j.msec.2020.111020
Received 8 January 2020; Received in revised form 24 April 2020; Accepted 25 April 2020
Available online 28 April 2020
0928-4931/ © 2020 Elsevier B.V. All rights reserved.

DNA adsorption studies have paid extremely attention in last years because of its wide set of good implementations in different areas. Adsorption of biomolecules can be affected by chemical and physical features of polymer surface used for operation [28]. Metal ion immobilization on nanoflowers can increase the interaction of them with biomolecules, which is wanted for applications in immobilized-metal ion affinity chromatography (IMAC) [29]. Even if different studies have been accomplished on DNA adsorption by different sources [7,30–33], there is no report for DNA adsorption with nanoflower by IMAC.

In this study, copper phosphate nanoflowers (CP-NFs) were synthesized, and Fe^{3+} ions were attached to surface of them to obtain Fe^{3+}-CP-NF. Fe^{3+}-CP-NFs were used as adsorbent to test IMAC effect of three dimensional nanoflowers for DNA adsorption. The characterization studies of Fe^{3+}-CP-NFs were evaluated based on the results of scanning electron microscopy (SEM), energy-dispersive X-ray (EDX), X-ray diffraction (XRD) and Fourier transform infrared spectroscopy (FTIR). To the best of our knowledge, inorganic Fe^{3+}-CP-NFs have been synthesized and used for separation of DNA molecules, first time. Because of no diffusion limitation between multi-layered nano-plates of flower-like matrix, a high separation capacity of DNA was reached. Fe^{3+}-CP-NFs are presented by our group to the literature as a promising inorganic nanomaterial for DNA adsorption.

2. Materials and methods

2.1. Material

All chemicals used in study were obtained from Sigma-Aldrich Inc. (St. Louis, MO, USA).

2.2. Methods

2.2.1. Preparation of copper phosphate nanoflowers (CP-NFs)

The CP-NFs were prepared by using a modified method [25,34]. First, 120 mM aqueous $CuSO_4$ stock solution and 10 mM phosphate buffered solution (PBS) (pH 7.4) were prepared. Then, certain amounts of $CuSO_4$ and PBS solutions were mixed. Final concentration of $CuSO_4$ was 0.8 mM. This mixture was vortexed to obtained homogeneous solution for 35–40 s and incubated at +4 °C for 3 days (Fig. 1). After incubation period, blue coloured precipitate [$Cu_3(PO_4)_2{\cdot}3H_2O$] occurred was collected by centrifugation (Nüve NF800R), washed with water at least three times to remove unreacted components, dried at room temperature, stored for further investigation and named as copper phosphate nanoflowers (CP-NFs).

2.2.2. Attachment of Fe^{3+} ions to copper phosphate nanoflowers (Fe^{3+}-CP-NFs)

Attachment of Fe^{3+} ions to CP-NFs was carried out at pH 4.7 (adjusted with 0.01 M HCl) in 150 ppm Fe^{3+} solution at room temperature. The binding procedure was conducted for 1 h. The concentration of Fe^{3+} ions in the medium was followed by inductively coupled plasma optical emission spectroscopy (ICP-OES) with a Varian Vista AX apparatus. Fe^{3+} ions incorporated to CP-NFs were determined by Eq. (1).

$$Q = (C_i - C_f)V/m \quad (1)$$

Here, C_i and C_f show starting and last Fe^{3+} concentrations (mg/mL) of the ions in the solution before and after attachment, respectively; Q symbolizes bound Fe^{3+} quantity onto CP-NFs (mg/g); V presents solution volume (mL) and m is quantity of CP-NFs (g). After the binding of Fe^{3+} ions, the example occurred was called as Fe^{3+}-CP-NFs.

Fe^{3+} leakage experiments from Fe^{3+}-CP-NFs were also studied in different medium with various pHs (4.0–7.0) including 1.0 M NaCl. For this purpose, Fe^{3+}-CP-NFs were mixed in the explained medium at room temperature for 1 day. The Fe^{3+} concentration in the solution was calculated by ICP-OES.

2.2.3. DNA adsorption experiments from aqueous solutions onto Fe^{3+}-CP-NFs

A rotator system (Stuart® SB3) was used for all adsorption and elution experiments. DNA adsorption experiments onto Fe^{3+}-CP-NFs were conducted with a gentle rotation at 20 rpm for 30 min with different buffer systems. It was performed in the range of pH 5.0–8.0 by using 0.05 M acetate buffer for pH 5.0–6.0 and 0.05 M MOPS (3-(N-morpholino) propanesulfonic acid) buffer for pH 7.0–8.0. DNA adsorption studies onto Fe^{3+}-CP-NFs were monitored at 260 nm. Optimum conditions for DNA adsorption studies were tested with some parameters such as initial concentration (0.2–2 mg/mL), pH (5.0–8.0), temperature (5–35 °C) and salt concentration effects (0–1 M NaCl). DNA adsorbed Fe^{3+}-CP-NFs were subjected to 1 M NaCl solution for elution of DNA at a rotation rate of 20 rpm for 30 min. The percentage of DNA eluted from Fe^{3+}-CP-NFs was provided between adsorbed and eluted DNA amounts.

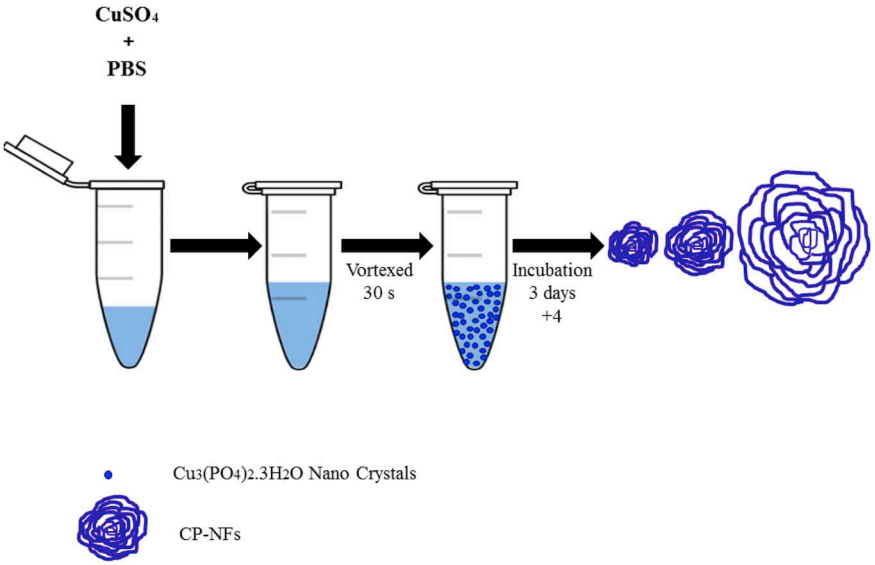


Fig. 1. Schematic representation of the synthesis the copper phosphate nanoflowers (CP-NFs).

2.2.4. Characterization of Fe^{3+}-CP-NFs

The morphology of the prepared CP-NFs was characterized by a scanning electron microscopy (SEM, Leo 440 computer controlled digital). The elemental composition of the CP-NFs was analyzed by using energy-dispersive X-ray (EDX, Leo 440 computer controlled digital). The crystal and the chemical structure of the CP-NFs were analyzed using X-ray diffraction (XRD, Bruker axs d8 advance model) and Fourier transform infrared spectroscopy (FTIR, Perkin Elmer 400, FTIR spectrometer spotlight 400 imaging system), respectively.

3. Results and discussion

In this study, inorganic nanoflowers (copper phosphate nanoflowers; CP-NFs) were synthesized and systematically characterized using some techniques (SEM, EDX, XRD and FTIR). The formation process of the CP-NFs is described in three steps; precipitation, transformation and self-assembly [25,34]. The formation of CP-NFs is shown in Fig. 2.

In the first step (the nucleation and formation of nanocrystals), when $CuSO_4$ solution is added into a PBS solution, bulk-like aggregates assembled from a large number of $Cu_3(PO_4)_2{\cdot}3H_2O$ nanocrystals are formed. In the second step (the growth of nanocrystals), with increasing the incubation time, the primary nanocrystals are continuously fed $Cu_3(PO_4)_2{\cdot}3H_2O$ nanocrystals to produce the large lamellar aggregates. In the final step (completion of CP-NFs), after incubation for 2–3 days, hierarchically and kinetically grown $Cu_3(PO_4)_2{\cdot}3H_2O$ nanocrystals reach the saturation level to complete the self-assembled process. At the end of the anisotropic growth process, almost all lamellar aggregates transform to CP-NFs, and the formation of CP-NFs is completed.

Luo et al. described the formation of copper phosphate nanoflowers without any organic small molecules (like amino acids) or macromolecules (like proteins or enzymes) [25]. They also reported some important parameters such as component of precursor solution, pH level, temperature and time on the growth mechanism of the copper phosphate nanoflowers. In this study, we prepared the CP-NFs at pH 7.4. To extend the application of the copper phosphate nanoflowers, which is different from the study given above, Fe^{3+} ions were immobilized on the CP-NFs. After immobilization, obtained Fe^{3+}-copper phosphate nanoflowers (Fe^{3+}-CP-NFs) were used for DNA separation.

3.1. Characterization studies for CP-NFs

The morphology of the synthesized CP-NFs was characterized by SEM (Fig. 3) via different magnifications. These figures reveal that the CP-NFs are consist of interconnected nano-plates. It is also clearly seen from Fig. 3 that CP-NFs have spherical shape and flower-like morphology. SEM images further confirm the high porous morphology of CP-NFs. Due to their porous nature, the CP-NFs have large surface area. Because of high surface to volume ratio, CP-NFs are highly suitable for biomolecule immobilization. Recently, flower-shaped materials (nanoflowers) have attracted increasing attention due to these fascinating features.

To investigate the chemical structure and elemental composition of the CP-NFs EDX, FTIR and XRD measurements were performed. The elemental distribution of Cu, O and P in EDX analysis and SEM-EDX mapping are given in Fig. 4A and B, respectively.

Energy dispersive X-ray (EDX) analysis indicated the presence of copper (Cu), oxygen (O) and phosphorus (P) elements in the synthesized CP-NFs. Elemental mapping results revealed that elements Cu, O and P were homogeneously distributed inside the CP-NFs.

The FTIR spectrum of the CP-NFs was examined as shown in Fig. 4C. In the FTIR spectrum, the peak at 1621 cm^{-1} came from the crystal water in copper phosphate three hydrate nanoflowers [$Cu_3(PO_4)_2{\cdot}3H_2O$, CP-NFs]. The peaks at ~1158 and ~1043 cm^{-1} were attributed to P═O and P−O vibrations, and the characteristic peaks at ~620 and ~566 cm^{-1} were attributed to O═P−O bending vibrations indicating the existence of phosphate groups.

XRD pattern of the CP-NFs (Fig. 4D) was consistent with that of $Cu_3(PO_4)_2{\cdot}3H_2O$ (JPSCD00-022-0548).

Amount of bound Fe^{3+} ions on CP-NFs was calculated to be 23 mg/g CP-NFs. Practised experiments after washing showed no Fe^{3+} ions leakage from CP-NFs.

3.2. DNA adsorption studies

In this episode of study, some adsorption parameters such as initial concentration, pH, ionic strength and temperature effects having importance in an adsorption process were come true. Oxygen species on phosphate groups in DNA structure have main responsibility for interaction with Fe^{3+} ions on CP-NFs. Some ions such as Fe^{3+}, Ga^{2+}, Al^{3+}, Ca^{2+} have more affinity for different groups like phosphate ones including oxygen moiety [35]. Among these ions, Fe^{3+} has much more affinity for phosphate groups [36]. In this study, as seen in Fig. 5A, the maximum DNA adsorption was occurred at pH 6 of 0.05 M acetate buffer. As known, net charge on DNA molecule is zero at pH 5 (isoelectric point of DNA) [37]. Because of hydroxylation and protonation possibilities of ligands (i.e., Fe^{3+} ions) on CP-NFs, upper and lower this pH, a repulsion could have come true between surface and DNA

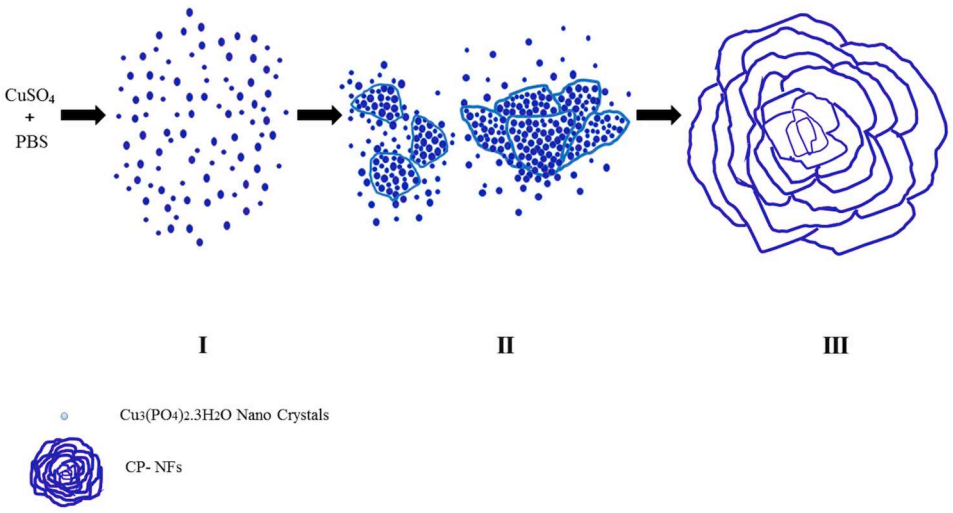


Fig. 2. The formation of the copper phosphate nanoflowers (CP-NFs): the nucleation and formation of nanocrystals (I); the growth of nanocrystals (II); completion of CP-NFs (III).

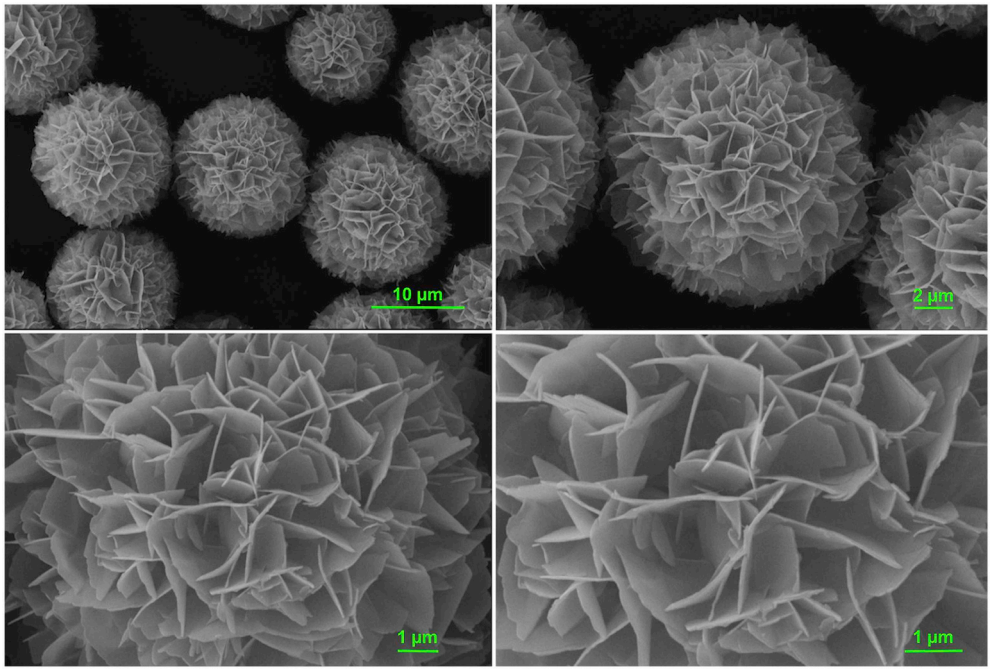


Fig. 3. SEM images of CP-NFs via different magnifications.

molecules [38,39]. And this situation can end up with lower adsorption [33].

As for initial DNA concentration effect on adsorption onto Fe^{3+}-CP-NFs, it was performed in the range of 0.25–2.0 mg DNA/mL, and obtained outcomes were given in Fig. 5B. As seen in this Figure, adsorption is reaching a plateau degree with DNA concentration of 1.5 mg/mL. While maximum adsorption was found to be 845.7 mg/g Fe^{3+}-CP-NFs, non-specific DNA adsorption for Fe^{3+} free CP-NFs was obtained as 25.4 mg/g. Attachment of Fe^{3+} ions remarkably increased the adsorption capacity of CP-NFs. Interaction phenomena between metal ions and biomolecules has some complexity. Electrostatic/ionic, hydrophobic and coordination interactions can be mentioned [40,41]. Coordination number and empty coordination sites of metal ions, medium pH and ionic strength, all play important role on interaction [42]. When metal ions are used as ligand in affinity chromatography, they can balance surface charge, which causes repulsion between adsorbent and

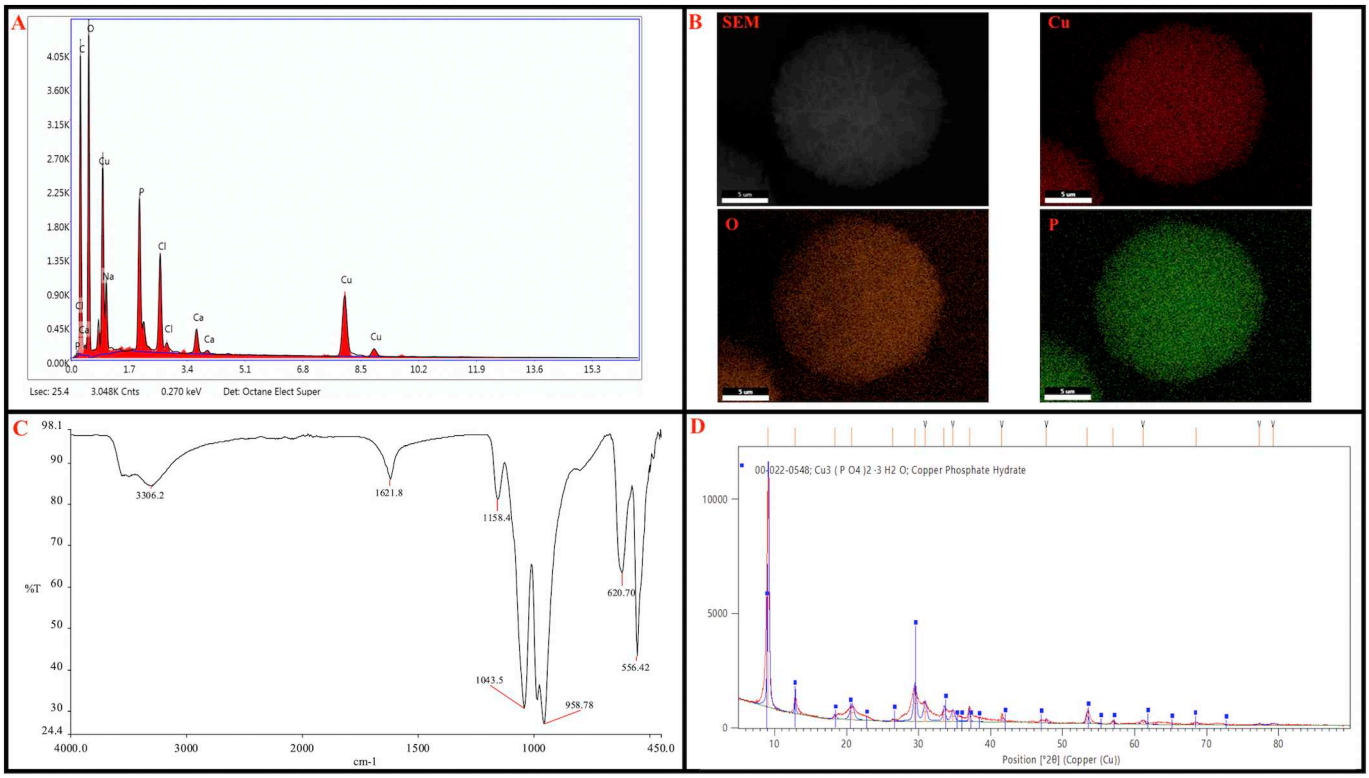


Fig. 4. Structure and elemental composition of the CP-NFs: A) EDX; B) SEM and EDX mapping images; C) FTIR spectrum; D) XRD patterns of CP-NFs.

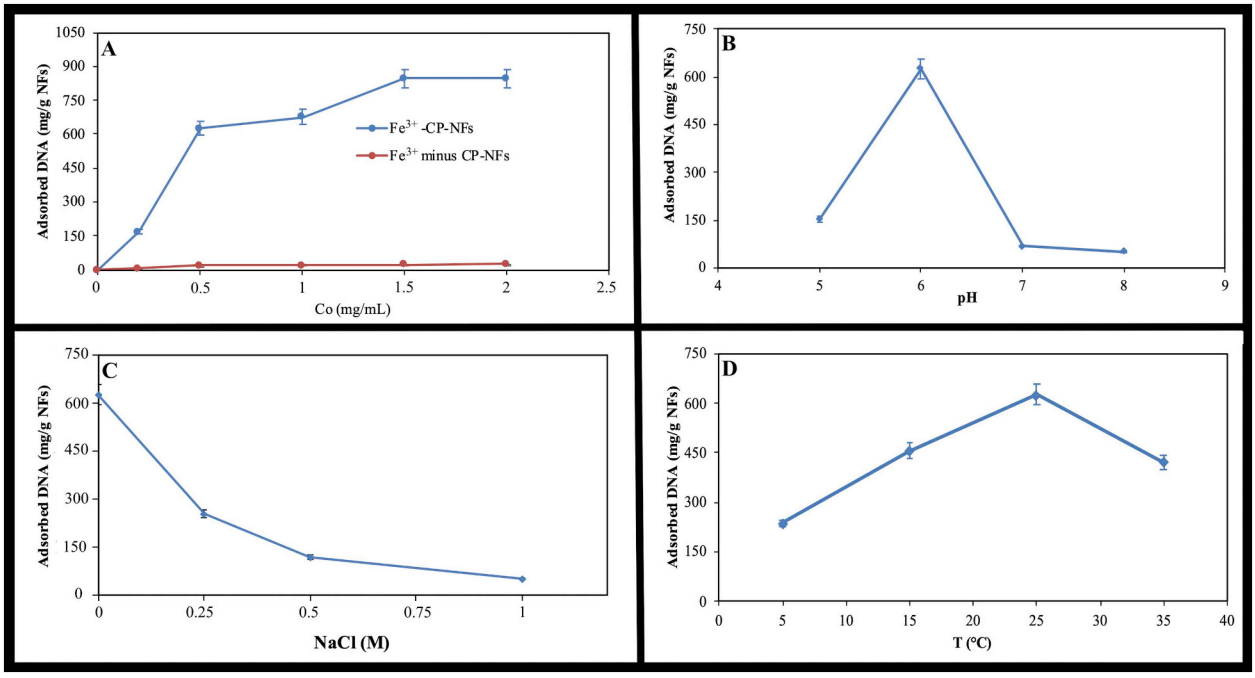


Fig. 5. Effect of medium parameters on DNA adsorption onto CP-NFs. (A) pH effect (C_{DNA}: 1 mg/mL, flow rate: 1 mL/min, T: 25 °C); (B) DNA concentration effect (pH 6.0, flow rate: 1 mL/min, T: 25 °C); (C) Ionic strength effect (pH 6.0, C_{DNA}: 1 mg/mL, flow rate: 1 mL/min, T: 25 °C); (D) Temperature effect (pH 6.0, C_{DNA}: 1 mg/mL, flow rate: 1 mL/min).

biomolecules. Reduction of surface repulsion effect results in enhancing of adsorption capacity [33,43]. It is known that Fe^{3+} ions have an affinity for DNA because of its phosphate structure including oxygen species [36]. A high adsorption amount of 845.7 mg/g Fe^{3+}-CP-NFs in this study can be attributed to both reduction of surface repulsion effect between NFs and DNA molecules and high surface area of nano-plates of CP-NFs.

IMAC matrix can acts an ion exchange material depending upon medium ionic strength [44]. Hence, ionic strength of medium may be used to manage the affinity of molecules in an adsorption process. In this study, ionic strength of medium was tested with NaCl ions in the range of 0–1.0 M, and results were given in Fig. 5C. As seen here, adsorption is decreasing with increased ionic strength of medium. Solved anionic and cationic ions in the medium can sheet opposite charges on the surface and adsorbed molecules. Hence, adsorption capability of biomolecules can be lowered [45].

In order to investigate the temperature activity in an adsorption process is also a necessary parameter. In IMAC, different interaction parameters (i.e., hydrophobic, electrostatic and/or coordination) depending on exposed functional groups of biomolecules (i.e., carboxyl, sulfhydryl, amine, etc.) are mentioned between metal ions and biomolecules in adsorption. Therefore, it is not easy to put forward which effect is dominance usually [44,46]. Here, temperatures effect on adsorption was researched in the range of 5–35 °C, and the highest DNA interaction was seen at 25 °C (Fig. 5D). Before and after this temperature, adsorption of DNA molecules on Fe^{3+}-CP-NFs was lower. This behaviour can be explained with dominant effect of ionic interaction at 25 °C.

The development of new adsorbents for separation of biomolecules is very important in the chromatographic area. Up to now, there are a lot of chromatographic media regarding their sorbent features such as cryogels [47], particles [48,49], biomaterials [50] embedded systems [2], etc. were offered in separation science. Especially, embedding systems were suggested as composed of two important features of sorbents like high surface area of particles and good flow rate of cryogels [51]. Nanoflowers have many combined features on them such as high surface area, high diffusion rate between nano-plates of flower like matrix, excessive adsorption capacity, etc. Some reports from literature regarding adsorption capacity for DNA were given in Table 1. As seen here, Fe^{3+}-CP-NFs have a crucial adsorption capacity.

Table 1
Comparison of DNA adsorption amount some adsorbents reported in the literature.

Adsorbents	Capacity (mg/g)	Ref.
IMAC application of sporopollenin particles	109	[2]
Fe^{3+} attached SBA-15 nanoparticles embedded column	751.5	[52]
Poly(hydroxyethyl methacrylate) based affinity cryogel	13.35	[47]
Zirconia magnetic nanocomposite	53.5	[48]
Cibacron Blue 3GA bound cryogel	32.5	[53]
Cu^{2+}-attached magnetite nanoparticles	19.97	[54]
DNA adsorption on different clay minerals	54.3	[55]
Ag^{+}-decorated poly(glycidyl methacrylate) microparticle	11.48	[56]
Silanized polymeric nanoparticles	672.41	[57]
Zn^{2+}-chelated poly(HEMA- MAH)] cryogel column	32.93	[58]
Poly(*N,N*-dimethylacrylamide)-grafted chitosan hydrogels	4.62	[59]
In this study	845.7	

3.3. Reusability studies

1 M NaCl solution prepared in pure water was used as elution medium of DNA molecules from Fe^{3+}-CP-NFs, and all parameters are results of triplicate measurements. From these results, it is noted that one sample used about 35 times without any remarkable losing from its adsorption performance. About only 3% losing was seen in adsorption capacity at the end of all experiments. In our previous study, pH 8 phosphate buffer including 1 M NaCl was used as elution medium for DNA adsorbed Fe^{3+} ion-attached matrix [33]. Here, pure water including 1 M NaCl ions was enough to elute DNA molecules. This result may be because of nano-plates of flower like cupper phosphate-based matrix.

Table 2
Obtained results and some remarkable properties of Langmuir and Freundlich isotherms.

Isotherm model	Related formula and linearized equations	Plots	Adsorption parameters	Isotherm values	Remarkable properties
Langmuir isotherm (related formula)	$Q_e = \frac{Q_m C_e}{K_d + C_e}$	C_e/Q_e vs C_e	Q_m K_d R^2 Equation	1000 (mg/g) 0.4 (mg/mL) 0.9885 $0.001\times + 4.10^{-4}$	• Occurrence of monolayer and energetically homogeneous adsorption phase by adsorbate. • Adsorbed molecules don't influence to each other. • Q_m: theoretical maximum adsorption. • Q_e: adsorbate in equilibrium. • K_d: dissociation constant
Langmuir isotherm (linearized equations)	$\frac{C_e}{Q_e} = \frac{C_e}{Q_m} + \frac{K_d}{Q_m}$				
Freundlich isotherm (related formula)	$Q_e = K_F C_e^{\frac{1}{n}}$	lnQ_e vs lnC_e	K_F n R^2 Equation	737.3 (mg/g) 1.9 0.9681 0.5269x + 6.603	• Monolayer (chemisorption) and multilayer adsorption (physisorption) possibilities can be mentioned for Freundlich isotherm regarding to surface heterogeneity and adsorbate. • n is indicator of adsorption intensity, • n < 1: when C_e increases, Q_e increases; • n > 1: Q_e stops even Ce increases.
Freundlich isotherm (linearized equations)	$ln\,Q_e = \frac{1}{n} ln\,C_e + ln\,K_F$				

3.4. DNA adsorption isotherm models

In order to investigate the distribution of adsorbed DNA molecules on the surface of Fe^{3+}-CP-NFs in equilibration state, two adsorption models such as Langmuir isotherm [60] and Freundlich isotherm [61], which are used mostly especially for adsorption of biomolecules. Obtained results and some remarkable properties of these models are given in Table 2. As seen from the correlation coefficients (R^2) extracted from equations, Langmuir model is more suitable than Freundlich one in point of R^2. Hence, it could be drawn a conclusion that Fe^{3+}-CP-NFs have a monolayer adsorption feature for DNA molecules.

4. Conclusions

Here, Fe^{3+}-CP-NFs without any organic components (as pure inorganic form) were synthesized, and some interaction parameters (i.e., effects of medium pH, initial concentration, ionic strength and temperature) regarding multi nano-plates of flower like copper phosphate-based matrix were evaluated for DNA separation. To the best of our knowledge, Fe^{3+}-CP-NFs have been used first time for separation of DNA as adsorbent. Because of no diffusion limitation between nano-plates of flower-like matrix, it was reached to a high adsorption value of 845.7 mg/g Fe^{3+}-CP-NFs with an initial DNA concentration of 1.5 mg/mL. pH 6 and temperature of 25 °C without any salt ions were found optimal conditions for DNA separation with Fe^{3+}-CP-NFs. When Langmuir and Freundlich adsorption isotherms were evaluated to check some kinetics adsorption processes, it was seen that Langmuir model with a correlation coefficient of 0.9885 was better for this system. Besides Fe^{3+} attached CP-NFs, Fe^{3+} minus CP-NFs were also tested for DNA separation, and it should be noted that a negligible amount of DNA molecules was adsorbed on CP-NFs surfaces as non-specific adsorption. Fe^{3+}-CP-NFs have still had their adsorption performance of 97% even at the end of 35-cycles. Under the light of all performed studies, it is hoped that Fe^{3+} attached copper phosphate nanoflowers (Fe^{3+}-CP-NFs) could be successfully implemented in the field of biotechnology and biomedicine with high amount of DNA separation.

CRediT authorship contribution statement

Ayça Serinbaş: Investigation.**Burcu Önal:**Investigation.**Ömür Acet:**Investigation.**Nalan Özdemir:**Conceptualization, Writing - review & editing.**Volha Dzmitruk:**Conceptualization.**Inessa Halets-Bui:**Investigation.**Dzmitry Shcharbin:**Conceptualization, Project administration, Funding acquisition, Writing - review & editing.**Mehmet Odabaşı:**Conceptualization, Project administration, Funding acquisition, Writing - review & editing.

Declaration of competing interest

On behalf of all authors, the corresponding author states that there is no conflict of interest.

Acknowledgements

This work was supported by the Technological Research Council of Turkey (TÜBITAK) (Grant Number: 118Z037) and by Belarusian Republican Foundation for Fundamental Research, grant B18TUB-001. Authors gratefully acknowledge use of the services and facilities of Technology Research and Implementation Center of Erciyes University (TAUM) and Scientific and Technological Application and Research Center of Aksaray University (ASUBTAM).

References

[1] S. Jiang, J. Zhuang, C. Wang, J. Li, W. Yang, Highly efficient adsorption of DNA on Fe^{3+}-iminodiacetic acid modified silica particles, Colloids Surf. A Physicochem. Eng. Asp. (2012), https://doi.org/10.1016/j.colsurfa.2012.05.051.
[2] Ş.C. Cömert, M. Odabaşi, Investigation of lysozyme adsorption performance of Cu2+-attached PHEMA beads embedded cryogel membranes, Mater. Sci. Eng. C (2014), https://doi.org/10.1016/j.msec.2013.09.033.
[3] R.J. Anderson, J. Schneider, Plasmid DNA and viral vector-based vaccines for the treatment of cancer, Vaccine (2007), https://doi.org/10.1016/j.vaccine.2007.05.030.
[4] J.A. Wolff, R.W. Malone, P. Williams, W. Chong, G. Acsadi, A. Jani, P.L. Felgner, Direct gene transfer into mouse muscle in vivo, Science (1990), https://doi.org/10.1126/science.1690918.
[5] D.C. Tang, M. Devit, S.A. Johnston, Genetic immunization is a simple method for eliciting an immune response, Nature (1992), https://doi.org/10.1038/356152a0.
[6] A.N. Butt, R. Swaminathan, Overview of circulating nucleic acids in plasma/serum, Ann. N. Y. Acad. Sci. (2009), https://doi.org/10.1196/annals.1448.002.
[7] X.Y. Sun, P.Z. Li, B. Ai, Y.B. Wang, Surface modification of MCM-41 and its application in DNA adsorption, Chin. Chem. Lett. 27 (2016) 139–144, https://doi.org/10.1016/j.cclet.2015.08.008.
[8] P. Shende, P. Kasture, R.S. Gaud, Nanoflowers: the future trend of nanotechnology for multi-applications, Artificial Cells, Nanomedicine, and Biotechnology 46 (2018) 413–422, https://doi.org/10.1080/21691401.2018.1428812.
[9] J. Ge, J. Lei, R.N. Zare, Protein-inorganic hybrid nanoflowers, Nat. Nanotechnol. (2012), https://doi.org/10.1038/nnano.2012.80.
[10] J. Cui, S. Jia, Organic–inorganic hybrid nanoflowers: a novel host platform for immobilizing biomolecules, Coord. Chem. Rev. (2017), https://doi.org/10.1016/j.ccr.2017.09.008.
[11] C. Altinkaynak, S. Tavlasoglu, R. Kalin, N. Sadeghian, H. Ozdemir, I. Ocsoy, N. Özdemir, A hierarchical assembly of flower-like hybrid Turkish black radish peroxidase-Cu^{2+} nanobiocatalyst and its effective use in dye decolorization, Chemosphere (2017), https://doi.org/10.1016/j.chemosphere.2017.05.012.
[12] E. Yilmaz, I. Ocsoy, N. Ozdemir, M. Soylak, Bovine serum albumin-Cu(II) hybrid nanoflowers: an effective adsorbent for solid phase extraction and slurry sampling flame atomic absorption spectrometric analysis of cadmium and lead in water, hair, food and cigarette samples, Anal. Chim. Acta (2016), https://doi.org/10.1016/j.aca.2015.12.001.
[13] M. Zahin, S. Hasan, F. Aqil, M.S.A. Khan, F.M. Husain, I. Ahmad, Screening of certain medicinal plants from India for their anti-quorum sensing activity, Indian J. Exp. Biol. 48 (2010) 1219–1224.

[14] I. Ali, Z.A. Al-Othman, A. Al-Warthan, Removal of secbumeton herbicide from water on composite nanoadsorbent, Desalin. Water Treat. (2016), https://doi.org/10.1080/19443994.2015.1041164.
[15] I. Ali, O.M.L. Alharbi, Z.A. Alothman, A.Y. Badjah, A. Alwarthan, A.A. Basheer, Artificial neural network modelling of amido black dye sorption on iron composite nano material: kinetics and thermodynamics studies, J. Mol. Liq. (2018), https://doi.org/10.1016/j.molliq.2017.11.163.
[16] A.A. Basheer, New generation nano-adsorbents for the removal of emerging contaminants in water, J. Mol. Liq. (2018), https://doi.org/10.1016/j.molliq.2018.04.021.
[17] X. Qi, X. Tong, T. Su, L. Lin, Q. Gong, Honeycomb-like hydrogel adsorbents derived from salecan polysaccharide for wastewater treatment, Cellulose (2019), https://doi.org/10.1007/s10570-019-02680-x.
[18] X. Qi, M. Chen, Y. Qian, M. Liu, Z. Li, L. Shen, T. Qin, S. Zhao, Q. Zeng, J. Shen, Construction of macroporous salecan polysaccharide-based adsorbents for wastewater remediation, Int. J. Biol. Macromol. (2019), https://doi.org/10.1016/j.ijbiomac.2019.03.155.
[19] X. Qi, R. Liu, M. Chen, Z. Li, T. Qin, Y. Qian, S. Zhao, M. Liu, Q. Zeng, J. Shen, Removal of copper ions from water using polysaccharide-constructed hydrogels, Carbohydr. Polym. (2019), https://doi.org/10.1016/j.carbpol.2019.01.015.
[20] X. Qi, L. Lin, L. Shen, Z. Li, T. Qin, Y. Qian, X. Wu, X. Wei, Q. Gong, J. Shen, Efficient decontamination of Lead ions from wastewater by salecan polysaccharide-based hydrogels, ACS Sustainable Chemistry and Engineering (2019), https://doi.org/10.1021/acssuschemeng.9b02139.
[21] L.B. Wang, Y.C. Wang, R. He, A. Zhuang, X. Wang, J. Zeng, J.G. Hou, A new nanobiocatalytic system based on allosteric effect with dramatically enhanced enzymatic performance, J. Am. Chem. Soc. (2013), https://doi.org/10.1021/ja3120136.
[22] D. Aydemir, F. Gecili, N. Özdemir, N. Nuray Ulusu, Synthesis and characterization of a triple enzyme-inorganic hybrid nanoflower (TrpE@ihNF) as a combination of three pancreatic digestive enzymes amylase, protease and lipase, J. Biosci. Bioeng. (2020), https://doi.org/10.1016/j.jbiosc.2020.01.008.
[23] Z. Lin, Y. Xiao, Y. Yin, W. Hu, W. Liu, H. Yang, Facile synthesis of enzyme-inorganic hybrid nanoflowers and its application as a colorimetric platform for visual detection of hydrogen peroxide and phenol, ACS Appl. Mater. Interfaces (2014), https://doi.org/10.1021/am502757e.
[24] J. Sun, J. Ge, W. Liu, M. Lan, H. Zhang, P. Wang, Y. Wang, Z. Niu, Multi-enzyme co-embedded organic-inorganic hybrid nanoflowers: synthesis and application as a colorimetric sensor, Nanoscale (2014), https://doi.org/10.1039/c3nr04425d.
[25] Y.K. Luo, F. Song, X.L. Wang, Y.Z. Wang, Pure copper phosphate nanostructures with controlled growth: a versatile support for enzyme immobilization, CrystEngComm (2017), https://doi.org/10.1039/c7ce00466d.
[26] Q. Ma, J. Liao, T. Tian, Q. Zhang, X. Cai, A potential flower-like coating consisting of calcium-phosphate nanosheets on titanium surface, Chin. Chem. Lett. (2017), https://doi.org/10.1016/j.cclet.2017.07.028.
[27] K.S. Park, B.S. Batule, M. Chung, K.S. Kang, T.J. Park, M. Il Kim, H.G. Park, A simple and eco-friendly one-pot synthesis of nuclease-resistant DNA-inorganic hybrid nanoflowers, J. Mater. Chem. B (2017), https://doi.org/10.1039/c6tb03047e.
[28] K. Nakanishi, T. Sakiyama, K. Imamura, On the adsorption of proteins on solid surfaces, a common but very complicated phenomenon, J. Biosci. Bioeng. (2001), https://doi.org/10.1016/S1389-1723(01)80127-4.
[29] E. Bulut, I. Sargin, O. Arslan, M. Odabasi, B. Akyuz, M. Kaya, In situ chitin isolation from body parts of a centipede and lysozyme adsorption studies, Mater. Sci. Eng. C (2017), https://doi.org/10.1016/j.msec.2016.08.048.
[30] M. Odabaşi, A. Denizli, Polyhydroxyethylmethacrylate-based magnetic DNA-affinity beads for anti-DNA antibody removal from systemic lupus erythematosus patient plasma, J. Chromatogr. B Biomed. Sci. Appl. (2001), https://doi.org/10.1016/S0378-4347(01)00264-X.
[31] M. Odabaşi, N. Özkayar, S. Özkara, S. Ünal, A. Denizli, Pathogenic antibody removal using magnetically stabilized fluidized bed, J. Chromatogr. B Anal. Technol. Biomed. Life Sci. (2005), https://doi.org/10.1016/j.jchromb.2005.08.004.
[32] C.H. Yang, P.W. Yang, T.L. Lin, U.S. Jeng, The adsorption of DNA by cationic core-shell diblock copolymer polystyrene-block-poly(N-methyl 4-vinylpyridine iodide) micelles, Colloids Surf. B: Biointerfaces (2019), https://doi.org/10.1016/j.colsurfb.2019.01.022.
[33] B. Önal, Ö. Acet, R. Sanz, E.S. Sanz-Pérez, D. Erdönmez, M. Odabaşı, Co-evaluation of interaction parameters of genomic and plasmid DNA for a new chromatographic medium, Int. J. Biol. Macromol. (2019), https://doi.org/10.1016/j.ijbiomac.2019.09.068.
[34] C. Gulmez, C. Altinkaynak, N. Özdemir, O. Atakisi, Proteinase K hybrid nanoflowers (P-hNFs) as a novel nanobiocatalytic detergent additive, Int. J. Biol. Macromol. (2018), https://doi.org/10.1016/j.ijbiomac.2018.07.195.
[35] V. Gaberc-Porekar, V. Menart, Perspectives of immobilized-metal affinity chromatography, J. Biochem. Biophys. Methods (2001), https://doi.org/10.1016/S0165-022X(01)00207-X.
[36] G. Muszyńska, G. Dobrowolska, A. Medin, A. Medin, P. Ekman, J.O. Porath, Model studies on iron(III) ion affinity chromatography. II.{star, open} interaction of immobilized iron(III) ions with phosphorylated amino acids, peptides and proteins, J. Chromatogr. A (1992), https://doi.org/10.1016/0021-9673(92)85524-W.
[37] G. Stotzky, Persistence and biological activity in soil of insecticidal proteins from Bacillus thuringiensis and of bacterial DNA bound on clays and humic acids, Journal of Environment Quality (2010), https://doi.org/10.2134/jeq2000.00472425002900030003x.
[38] P. Jerker, Amino acid side chain interaction with chelate-liganded crosslinked dextran, agarose and TSK gel. A mini review of recent work, J. Mol. Recognit. (2004), https://doi.org/10.1002/jmr.300030306.
[39] J.R. Sosa-Acosta, J.A. Silva, L. Fernández-Izquierdo, S. Díaz-Castañón, M. Ortiz, J.C. Zuaznabar-Gardona, A.M. Díaz-García, Iron oxide nanoparticles (IONPs) with potential applications in plasmid DNA isolation, Colloids Surf. A Physicochem. Eng. Asp. (2018), https://doi.org/10.1016/j.colsurfa.2018.02.062.
[40] K.A. Melzak, C.S. Sherwood, R.F.B. Turner, C.A. Haynes, Driving forces for DNA adsorption to silica in perchlorate solutions, J. Colloid Interface Sci. (1996), https://doi.org/10.1006/jcis.1996.0421.
[41] F. Gurbuz, Ş. Ceylan, M. Odabaşi, G.A. Codd, Hepatotoxic microcystin removal using pumice embedded monolithic composite cryogel as an alternative water treatment method, Water Res. (2016), https://doi.org/10.1016/j.watres.2015.12.042.
[42] L. Beltran, P.R. Cutillas, Advances in phosphopeptide enrichment techniques for phosphoproteomics, Amino Acids (2012), https://doi.org/10.1007/s00726-012-1288-9.
[43] T.H. Nguyen, M. Elimelech, Plasmid DNA adsorption on silica: kinetics and conformational changes in monovalent and divalent salts, Biomacromolecules (2007), https://doi.org/10.1021/bm0603948.
[44] Ö. Acet, N.H. Aksoy, D. Erdönmez, M. Odabaşı, Determination of some adsorption and kinetic parameters of α-amylase onto Cu+2-PHEMA beads embedded column, artificial cells, Nanomedicine and Biotechnology (2018), https://doi.org/10.1080/21691401.2018.1501378.
[45] N.Y. Baran, Ö. Acet, M. Odabaşı, Efficient adsorption of hemoglobin from aqueous solutions by hybrid monolithic cryogel column, Mater. Sci. Eng. C (2017), https://doi.org/10.1016/j.msec.2016.12.036.
[46] S. Sharma, G.P. Agarwal, Interactions of proteins with immobilized metal ions: a comparative analysis using various isotherm models, Anal. Biochem. (2001), https://doi.org/10.1006/abio.2000.4894.
[47] I. Perçin, E. Saĝlar, H. Yavuz, E. Aksöz, A. Denizli, Poly(hydroxyethyl methacrylate) based affinity cryogel for plasmid DNA purification, Int. J. Biol. Macromol. (2011), https://doi.org/10.1016/j.ijbiomac.2011.01.022.
[48] M. Saraji, S. Yousefi, M. Talebi, Plasmid DNA purification by zirconia magnetic nanocomposite, Anal. Biochem. (2017), https://doi.org/10.1016/j.ab.2017.10.004.
[49] H. Yavuz, M. Odabaşi, S. Akgöl, A. Denizli, Immobilized metal affinity beads for ferritin adsorption, J. Biomater. Sci. Polym. Ed. (2005), https://doi.org/10.1163/1568562053783713.
[50] M. Kaya, M. Odabasi, M. Mujtaba, M. Sen, E. Bulut, B. Akyuz, Novel three-dimensional cellulose produced from trunk of Astragalus gummifer (Fabaceae) tested for protein adsorption performance, Mater. Sci. Eng. C (2016), https://doi.org/10.1016/j.msec.2016.01.047.
[51] Ö. Acet, T. Baran, D. Erdönmez, N.H. Aksoy, İ. Alacabey, A. Menteş, M. Odabaşi, O-carboxymethyl chitosan Schiff base complexes as affinity ligands for immobilized metal-ion affinity chromatography of lysozyme, J. Chromatogr. A (2018), https://doi.org/10.1016/j.chroma.2018.03.022.
[52] Ö. Acet, B. Önal, R. Sanz, E.S. Sanz-Pérez, D. Erdönmez, M. Odabaşi, Preparation of a new chromatographic media and assessment of some kinetic and interaction parameters for lysozyme, J. Mol. Liq. (2019), https://doi.org/10.1016/j.molliq.2018.12.037.
[53] D. Çimen, F. Yilmaz, I. Perçin, D. Türkmen, A. Denizli, Dye affinity cryogels for plasmid DNA purification, Mater. Sci. Eng. C (2015), https://doi.org/10.1016/j.msec.2015.06.041.
[54] Ş. Ceylan, T. Kalburcu, M. Gedikli, M. Odabaşı, Application of Cu2+-attached magnetite nanoparticles embedded supermacroporous monolithic composite cryogels for DNA adsorption, Hacett J Bio Chem 39 (2011) 163–172.
[55] P. Cai, Q. Huang, X. Zhang, H. Chen, Adsorption of DNA on clay minerals and various colloidal particles from an Alfisol, Soil Biol. Biochem. (2006), https://doi.org/10.1016/j.soilbio.2005.05.019.
[56] K. Erol, A. Uzunoglu, K. Köse, B. Sarıca, E. Avcı, D.A. Köse, Synthesis and characterization of Ag+-decorated poly(glycidyl methacrylate) microparticle design for the adsorption of nucleic acids, J. Chromatogr. B Anal. Technol. Biomed. Life Sci. (2018), https://doi.org/10.1016/j.jchromb.2018.02.017.
[57] C. Türkcan, S. Akgöl, A. Denizli, Silanized polymeric nanoparticles for DNA isolation, Mater. Sci. Eng. C (2013), https://doi.org/10.1016/j.msec.2013.05.015.
[58] M. Odabaşi, G. Baydemir, M. Karataş, A. Derazshamshir, Preparation and characterization of metal-chelated poly(HEMA-MAH) monolithic cryogels and their use for DNA adsorption, J. Appl. Polym. Sci. (2010), https://doi.org/10.1002/app.31505.
[59] B. Başer, G.B. Demirel, T. Caykara, DNA adsorption on poly(N,N-dimethylacrylamide)-grafted chitosan hydrogels, J. Appl. Polym. Sci. (2011), https://doi.org/10.1002/app.33029.
[60] I. Langmuir, The adsorption of gases on plane surfaces of glass, mica and platinum, J. Am. Chem. Soc. (1918), https://doi.org/10.1021/ja02242a004.
[61] H.M.F. Freundlich, Over the adsorption in solution, J. Phys. Chem. (1906), https://doi.org/10.4236/jep.2017.84030.